

Deep Feature Screening: Feature Selection for Ultra High-Dimensional Data via Deep Neural Networks

KEXUAN LI*

Department of Mathematical Sciences, Worcester Polytechnic Institute

kli6@wpi.edu

FANGFANG WANG

Department of Mathematical Sciences, Worcester Polytechnic Institute

fwang4@wpi.edu

LINGLI YANG

Department of Mathematical Sciences, Worcester Polytechnic Institute

lyang8@wpi.edu

SUMMARY

The applications of traditional statistical feature selection methods to high-dimension, low-sample-size data often struggle and encounter challenging problems, such as overfitting, curse of dimensionality, computational infeasibility, and strong model assumption. In this paper, we propose a novel two-step nonparametric approach called Deep Feature Screening (DeepFS) that can overcome these problems and identify significant features with high precision for ultra high-

*Corresponding author

dimensional, low-sample-size data. This approach first extracts a low-dimensional representation of input data and then applies feature screening based on multivariate rank distance correlation recently developed by Deb and Sen (2021). This approach combines the strengths of both deep neural networks and feature screening, and thereby has the following appealing features in addition to its ability of handling ultra high-dimensional data with small number of samples: (1) it is model free and distribution free; (2) it can be used for both supervised and unsupervised feature selection; and (3) it is capable of recovering the original input data. The superiority of DeepFS is demonstrated via extensive simulation studies and real data analyses.

Key words: Deep Neural Networks; Ultra High-Dimensional Data; Feature Selection; Feature Screening; Dimension Reduction.

1. INTRODUCTION

(Ultra) high-dimensional data are commonly encountered in research areas such as machine learning, computer vision, financial engineering, and biological science. In statistical and machine learning literatures, people use high dimensionality to refer to the case where the dimensionality p grows to infinity, while the ultra-high dimensionality means that the dimensionality p grows at a non-polynomial rate of sample size n (say, $p = O(\exp(n^\xi))$ for some $\xi > 0$); see Fan and Lv (2008) and Fan et al. (2009). To analyze (ultra) high-dimensional data, feature selection has been regarded as a powerful tool to achieve dimension reduction, in that a significant amount of features are irrelevant and redundant in many problems of interest. Correctly selecting a representative subset of features plays an important role in these applications. For example, in genome-wide association studies (GWAS), researchers are interested in identifying genes that contain single-nucleotide polymorphisms (SNPs) associated with target human diseases. GWAS datasets oftentimes contain a large number of SNPs (e.g., $p \geq 10^5$), but the sample size n is

quite small (e.g., $n \leq 10^3$). It is well known that the selection of an optimal subset is an NP-hard problem (Amaldi and Kann, 1998). Thus, a vast amount of feature selection methods have been proposed to address this problem.

Based on the interaction of feature selection search and the learning model, the traditional feature selection methods can be broadly categorized into three classes: filter methods, wrapper methods, and embedded methods. The filter methods require features to be selected according to certain statistical measure such as information gain, chi-square test, fisher score, correlation coefficient, and variance threshold. In the wrapper methods, features are selected based on a classifier; some commonly adopted classifiers include recursive feature elimination, sequential feature selection algorithms, and genetic algorithms. The embedded methods use ensemble learning and hybrid learning methods for feature selection. See Saeys et al. (2007), Kabir et al. (2011), Chandrashekar and Sahin (2014), Khalid et al. (2014), Miao and Niu (2016), Mohsenzadeh et al. (2016), and Mirzaei et al. (2017) for more detail on the three methods. However, these classical methods suffer from some potential problems when applied to ultra high-dimensional data. For example, they ignore feature dependence and nonlinear structure, lack flexibility, and require a large sample size. When implementing these methods, people tend to assume a parametric form (like linear model and logistic regression model) to describe the relationship between the response and the features and ignore the interactions among features, which, however, can be complex and nonlinear in practice (Wu et al., 2009; Yang et al., 2020). Despite that both supervised and unsupervised feature selections have important applications, most algorithms cannot combine supervised and unsupervised learnings effectively (see Ding, 2003; Varshavsky et al., 2006; Qi et al., 2018; Zhu et al., 2018; Taherkhani et al., 2018; Solorio-Fernández et al., 2020). The successful application of feature selection algorithms to high-dimensional data relies on a large sample size. However, when dealing with high-dimension, low-sample-size data, such methods suffer from computational instability in addition to curse of dimensionality and overfitting.

To overcome these problems, we propose an effective feature selection approach based on deep neural network and feature screening, called DeepFS, under ultra-high-dimension, small-sample-size setup with only a few tuning parameters. Our method enjoys several advantages: (1) it can be used for both supervised and unsupervised feature selection; (2) it is distribution-free and model-free; (3) it can capture nonlinear and interaction among features; (4) it can provide an estimation of the number of active features. To be more specific, our feature selection procedure consists of two steps: feature extraction and feature screening. In the first step, we use an autoencoder or supervised autoencoder to extract a good representation of data. In the second step, we screen each feature and the low-dimensional representation generated from the first step and compute the corresponding importance score associated with each feature via multivariate rank distance correlation. The features with high importance scores will then be selected. Apparently, this two-step method shares both advantages of deep learning and feature screening. To the best of our knowledge, this study is the first attempt to combine deep neural networks and feature screening.

The rest of the paper is organized as follows. In Section 2, we formulate the problem of interest and briefly review the feature screening and feature selection in deep learning literature. We introduce our method in Section 3 and comprehensive simulation studies are presented in Section 4. In Section 5, we apply DeepFS to some real-world datasets and give our conclusion in Section 6.

2. PROBLEM FORMULATION AND RELATED WORKS

In this section, we formulate the problem under study, followed by a literature review of feature selection methods by means of feature screening and deep learning.

2.1 Problem Formulation

We first describe the problems often encountered in unsupervised feature selection and supervised feature selection. Suppose there are n observations $\mathbf{x}_i \in \mathbb{R}^p, i = 1, \dots, n$, where p is the number of features, that are independent and identically distributed (*i.i.d.*) from distribution $p(\mathbf{x}), \mathbf{x} \in \mathbb{R}^p$. In unsupervised feature selection, the goal is to identify a subset $\mathcal{S} \subseteq \{1, 2, \dots, p\}$ of the most discriminative and informative features with size $|\mathcal{S}| = k \leq p$ and also a reconstruction function $g : \mathbb{R}^k \rightarrow \mathbb{R}^p$ from a low dimensional feature space \mathbb{R}^k to the original feature space \mathbb{R}^p , such that the expected loss between $g(\mathbf{x}^{(\mathcal{S})})$ and the original input $\mathbf{x} \in \mathbb{R}^p$ is minimized, where $\mathbf{x}^{(\mathcal{S})} = (x_{s_1}, \dots, x_{s_k})^\top \in \mathbb{R}^k$ and $s_i \in \mathcal{S}$. In supervised feature selection, people not only know the sample design matrix $(\mathbf{x}_1, \dots, \mathbf{x}_n)^\top \in \mathbb{R}^{n \times p}$, but also the label vector $\mathbf{y} = (y_1, \dots, y_n)^\top \in \mathbb{R}^n$, where y_i can be continuous or categorical. Suppose that the true relationship between a subset of features, \mathcal{S} , and the label is such that $y_i = f(\mathbf{x}_i^{(\mathcal{S})})$, with $\mathbf{x}_i^{(\mathcal{S})} = (x_{i,s_1}, \dots, x_{i,s_k})^\top, s_i \in \mathcal{S}, i = 1, \dots, n$. For example, we can assume $f(\cdot)$ has a parametric linear form: $y_i = f(\mathbf{x}_i^{(\mathcal{S})}) = \beta_0 + \sum_{j=1}^k \beta_j x_{i,s_j} + \epsilon_i$ for continuous response or logistic regression $\log \frac{Pr(y_i=1)}{Pr(y_i=0)} = \beta_0 + \sum_{j=1}^k \beta_j x_{i,s_j}$ for categorical response. However, the linearity assumption is too stringent in real world applications and thus we should consider more flexible choices for $f(\cdot)$, such as neural networks.

2.2 Related Works

The literature on feature selection is vast and encompasses many fields. In this subsection, we do not provide a comprehensive review here, but rather focus on popular methods in feature screening and deep learning instead. We refer the reader to Kumar and Minz (2014) for a more in-depth review of the classical feature selection literature.

Feature screening is a fundamental problem in the analysis of ultra high-dimensional data. To be specific, feature screening is a process of assigning a numerical value, known as importance score, to each feature according to a certain statistical measure that quantifies the strength of

dependence between the feature and the response, and then ranking the importance scores and selecting the top k features accordingly. The statistical measure can be Pearson correlation (Fan and Lv, 2008) and distance correlation (Li et al., 2012), among others. A good feature screening method should enjoy the theoretical property called *sure screening property*, meaning that all the true features can be selected with probability approaching to one as the sample size goes to infinity. It is worth mentioning that Deb and Sen (2021) proposes a novel test statistic called multivariate rank distance correlation that makes it possible to carry out a model-free nonparametric procedure to test mutual independence between random vectors in multi-dimensions. Zhao and Fu (2021) apply the test statistic of Deb and Sen (2021) to feature screening and introduce a distribution-free nonparametric screening approach called MrDc-SIS that is proved to be asymptotic sure screening consistency. However, similar to other feature screening methods, MrDc-SIS has several drawbacks: (1) It ignores the reconstruction of original inputs; (2) It does not consider inter-dependence among the features; (3) It is not trivial to extend MrDc-SIS to unsupervised feature selection or supervised feature selection with categorical responses. Thus, MrDc-SIS is of limited effectiveness.

In recent years, deep learning has made a great breakthrough in both theory and practice. In particular, Liu et al. (2020); Schmidt-Hieber (2020); Liu et al. (2022) proves that deep neural networks can achieve the minimax rate of convergence in a nonparametric setting under some mild conditions. Farrell et al. (2021) studies the rates of convergence for deep feedforward neural nets in semiparametric inference. The successful applications include, but are not limited to, computer vision (He et al., 2016), natural language processing (Bahdanau et al., 2014), drug discovery and toxicology (Jiménez-Luna et al., 2020), and dynamics system (Li et al., 2021), functional data analysis (Wang et al., 2021).

Applying deep learning to feature selection has also gained much attention. For example, deep feature selection (DFS) of Li et al. (2016) learns one-to-one connections between input features

and the first hidden layer nodes. Using a similar idea, Liu et al. (2017) proposes a so-called deep neural pursuit (DNP) that selects relevant features by averaging out gradients with lower variance via multiple dropouts. However, both DFS and DNP ignore the reconstruction of original input and use only a simple multi-layer perceptron, which fail to capture the complex structure.

Another technique commonly used in deep learning for feature selection is reparametrization trick, or Gumbel-softmax trick (Jang et al., 2016). For example, Abid et al. (2019) and Singh et al. (2020) consider a concrete selector layer such that the gradients can pass through the network for discrete feature selection. By using reparametrization trick, the network can stochastically select a linear combination of inputs and converge to a discrete subset of features in the end. However, caution is called for when one uses concrete random variable for discrete feature selection. First, the performance is very sensitive to the tuning parameters. Second, because the concrete selector layer stochastically searches k out of p features, where k is predetermined representing the number of features one desires to select, the probability of concrete selector layer picking up correct features is very small when p is large relative to k . Third, successfully training concrete selector layer requires a huge amount of samples, which is infeasible under high-dimension, low-sample-size setting.

Recently, Lemhadri et al. (2021) introduces a new feature selection framework for neural networks called LassoNet by adding a residual layer from the input layer to the output, penalizing the parameters in the residual layer, and imposing a constraint that the norm of the parameters in the first layer is less than the corresponding norm of the parameters in the residual layer. The authors have demonstrated that LassoNet “significantly outperforms state-of-the-art methods for feature selection and regression”. In this paper, we will show through both simulations and real data analyses that our proposed method performs even better than LassoNet, especially when the sample size is small (see Sections 4 and 5).

The study by Mirzaei et al. (2020) considers a teacher-student scheme for feature selection.

In the teacher step, a sophisticated network architecture is used in order to capture the complex hidden structure of the data. In the student step, the authors use a single-layer feed-forward neural network with a row-sparse regularization to mimic the low-dimensional data generated from the teacher step and then perform feature selection. The idea of adding row-sparse regularization to hidden layers in feature selection is not new (e.g., Scardapane et al., 2017; Han et al., 2018; Feng and Duarte, 2018). However, when dealing with high-dimension, low-sample-size data, these techniques fail to select correct features because of overfitting and high-variance gradients. Moreover, their performance is very sensitive to the regularization parameters.

3. METHODS

In this section, we provide the details of our method. It consists of two step. In Step 1, we use autoencoder to extract a low-dimensional representation of the original data and this is known as feature extraction step, while in Step 2, we apply feature screening via multivariate rank distance correlation learning to achieve feature selection.

3.1 Step 1: Dimension Reduction and Feature Extraction

In the first step, we use an autoencoder to learn a complex representation of the input data. Autoencoder is one type of feed-forward neural networks, and is commonly used for dimension reduction. A standard (unsupervised) autoencoder consists of two parts, the encoder and the decoder. Suppose both the input space and output space is \mathcal{X} and the hidden layer space is \mathcal{F} . Throughout the paper, we assume $\mathcal{X} = \mathbb{R}^p$ and $\mathcal{F} = \mathbb{R}^h$. The goal is to find two maps $\Phi : \mathcal{X} \rightarrow \mathcal{F}$ and $\Psi : \mathcal{F} \rightarrow \mathcal{X}$ that minimize the reconstruction loss function $\mathcal{L}_r(\Theta|\mathbf{x}) = n^{-1} \sum_{i=1}^n \|\mathbf{x}_i - \Psi(\Phi(\mathbf{x}_i))\|_2^2$, where $\Theta = [\Theta_\Phi, \Theta_\Psi]$ collects all the model parameters and $\|\cdot\|_2$ is the l_2 norm. Here, we refer to Φ as encoder and Ψ as decoder. To better learn the possibly nonlinear structure of the features, we assume that Φ and Ψ are neural networks. For example, suppose that there

is only one layer in both encoder and decoder; then for $\mathbf{x} \in \mathcal{X}$, $\Phi(\mathbf{x}) = \sigma(\mathbf{W}\mathbf{x} + b) \in \mathcal{F}$, $\Psi(\Phi(\mathbf{x})) = \sigma'(\mathbf{W}'\Phi(\mathbf{x}) + b')$, and

$$\mathcal{L}_r(\Theta|\mathbf{x}) = \frac{1}{n} \sum_{i=1}^n \|\mathbf{x}_i - \Psi(\Phi(\mathbf{x}_i))\|_2^2 = \frac{1}{n} \sum_{i=1}^n \|\mathbf{x}_i - \sigma'(\mathbf{W}'\sigma(\mathbf{W}\mathbf{x}_i + b) + b')\|_2^2, \quad (3.1)$$

where $\sigma(), \sigma'()$ are nonlinear active functions, \mathbf{W}, \mathbf{W}' are weight matrices, and b, b' are bias vectors. The standard autoencoder can be replaced with its variants, such as sparse autoencoder, denoising autoencoder, and variational autoencoder.

When it comes to supervised feature selection, we use a supervised autoencoder instead of the standard (unsupervised) autoencoder. In supervised autoencoder, we add an additional loss on the hidden layer, such as the mean square loss for continuous response or the cross-entropy loss for categorical response. Let $\mathcal{L}_s(\cdot)$ be the supervised loss on the hidden layer and $\mathcal{L}_r(\cdot)$ be the reconstruction loss as in Equation (3.1). The loss for supervised autoencoder with continuous response is:

$$\begin{aligned} \mathcal{L}(\Theta|\mathbf{x}, y) &= \mathcal{L}_s(\Theta_\Phi, \Theta_\Upsilon|\mathbf{x}, y) + \lambda \mathcal{L}_r(\Theta_\Phi, \Theta_\Psi|\mathbf{x}) \\ &= \frac{1}{n} \sum_{i=1}^n (\|y_i - \Upsilon(\Phi(\mathbf{x}_i))\|_2^2 + \lambda \|\mathbf{x}_i - \Psi(\Phi(\mathbf{x}_i))\|_2^2), \end{aligned} \quad (3.2)$$

where $y \in \mathcal{Y}$, $\Theta = [\Theta_\Phi, \Theta_\Psi, \Theta_\Upsilon]$ is the model parameters, $\Upsilon : \mathcal{F} \rightarrow \mathcal{Y}$ is the regressor, and λ is the tuning parameter controlling the strength of the reconstruction loss. It is worth mentioning that while in classical feature selection method $\mathcal{Y} = \mathbb{R}$, in our setting, \mathcal{Y} could be a more general space, like \mathbb{R}^k for some integer k greater than 1. The corresponding loss in the supervised autoencoder with categorical response becomes:

$$\begin{aligned} \mathcal{L}(\Theta|\mathbf{x}, y) &= \mathcal{L}_s(\Theta_\Phi, \Theta_\Upsilon|\mathbf{x}, y) + \lambda \mathcal{L}_r(\Theta_\Phi, \Theta_\Psi|\mathbf{x}) \\ &= \frac{1}{n} \sum_{i=1}^n \left(-\log \left(\frac{\exp(\Upsilon(\mathbf{x}_i)_{y_i})}{\sum_{c=1}^C \exp(\Upsilon(\mathbf{x}_i)_c)} \right) + \lambda \|\mathbf{x}_i - \Psi(\Phi(\mathbf{x}_i))\|_2^2 \right), \end{aligned} \quad (3.3)$$

where Θ, Φ, Ψ and λ are the same as Equation (3.2), C is the number of classes, and $\Upsilon : \mathcal{F} \rightarrow \mathbb{R}^C$ is a classifier on the hidden layer with softmax output.

The training process in the first step is an optimization problem, i.e., minimizing $\mathcal{L}(\Theta|\mathbf{x}, y)$. Once the model is trained, we can extract a subset of features by mapping the original inputs

from \mathcal{X} to the low dimensional hidden space \mathcal{F} . Precisely speaking, we define the normalized encoded input

$$\mathbf{x}_{\text{encode}} = \frac{\Phi(\mathbf{x}) - \min_{\mathbf{x} \in \mathcal{X}} \Phi(\mathbf{x})}{\max_{\mathbf{x} \in \mathcal{X}} \Phi(\mathbf{x}) - \min_{\mathbf{x} \in \mathcal{X}} \Phi(\mathbf{x})} \in \mathcal{F},$$

which generates the abstract features from the original high dimensional data and will be used later in the second step.

3.2 Step 2: Feature Screening

With the aid of the low-dimensional representation of the high-dimensional features generated from the first step, in the second step, we screen all the features via multivariate rank distance correlation learning to select the relevant ones. Unlike Mirzaei et al. (2020) which uses a single-layer feed forward network with row-sparse regularization to mimic the data generated from the first step, we screen $\mathbf{x}_{\text{encoded}}$ with respect to each feature. The reason for using feature screening instead of neural network is the small amount of training samples. When training samples are limited, neural network can easily result in overfitting; however, if we only consider one feature at a time, the dependence between the feature and $\mathbf{x}_{\text{encoded}}$ can still be well estimated even the sample size is small.

The feature screening procedure via multivariate rank distance correlation has been proved to be of asymptotic sure screening consistency by Zhao and Fu (2021). For the sake of convenience, in what follows, we recapitulate the multivariate rank distance correlation of Deb and Sen (2021).

We start by introducing the multivariate rank. Let $\{\mathbf{c}_1, \dots, \mathbf{c}_n\} \subset [0, 1]^p$ be a “uniform-like” quasi-Monte Carlo sequence on $[0, 1]^p$ such as Halton sequences (Halton and Smith, 1964), Sobol sequence (Sobol’, 1967), and equally-spaced p -dimensional lattice. Given *i.i.d.* random vectors $\mathbf{X}_1, \dots, \mathbf{X}_n \in \mathbb{R}^p$ and consider the following optimization problem:

$$\hat{\sigma} = \arg \min_{\sigma=(\sigma(1), \dots, \sigma(n)) \in S_n} \sum_{i=1}^n \|\mathbf{X}_i - \mathbf{c}_{\sigma(i)}\|^2 = \arg \max_{\sigma=(\sigma(1), \dots, \sigma(n)) \in S_n} \sum_{i=1}^n \langle \mathbf{X}_i, \mathbf{c}_{\sigma(i)} \rangle, \quad (3.4)$$

where $\|\cdot\|$ and $\langle \cdot, \cdot \rangle$ denote the usual Euclidean norm and inner product, and S_n is the set of all permutations of $\{1, 2, \dots, n\}$. The (empirical) multivariate rank of \mathbf{X}_i is a p -dimensional vector defined as

$$\text{Rank}(\mathbf{X}_i) = \mathbf{c}_{\hat{\sigma}(i)}, \quad \text{for } i = 1, \dots, n. \quad (3.5)$$

Figure 1 illustrates the idea of multivariate rank on $[0, 1]^2$.

The rank distance covariance is defined as a measure of mutual dependence. Suppose that $\{\mathbf{X}_1, \dots, \mathbf{X}_n\}$ and $\{\mathbf{Y}_1, \dots, \mathbf{Y}_n\}$ are samples of n observations from p -dimensional random vector \mathbf{X} and q -dimensional random vector \mathbf{Y} , respectively. The (empirical) rank distance covariance and rank distance correlation between \mathbf{X} and \mathbf{Y} are defined as

$$\text{RdCov}^2(\mathbf{X}, \mathbf{Y}) = S_1 + S_2 - 2S_3, \quad \text{RdCorr}(\mathbf{X}, \mathbf{Y}) = \frac{\text{RdCov}(\mathbf{X}, \mathbf{Y})}{\sqrt{\text{RdCov}(\mathbf{X}, \mathbf{X})\text{RdCov}(\mathbf{Y}, \mathbf{Y})}} \quad (3.6)$$

respectively, where

$$\begin{aligned} S_1 &= \frac{1}{n^2} \sum_{k,l=1}^n \|\text{Rank}(\mathbf{X}_k) - \text{Rank}(\mathbf{X}_l)\| * \|\text{Rank}(\mathbf{Y}_k) - \text{Rank}(\mathbf{Y}_l)\|, \\ S_2 &= \left(\frac{1}{n^2} \sum_{k,l=1}^n \|\text{Rank}(\mathbf{X}_k) - \text{Rank}(\mathbf{X}_l)\| \right) * \left(\frac{1}{n^2} \sum_{k,l=1}^n \|\text{Rank}(\mathbf{Y}_k) - \text{Rank}(\mathbf{Y}_l)\| \right), \\ S_3 &= \frac{1}{n^3} \sum_{k,l,m=1}^n \|\text{Rank}(\mathbf{X}_k) - \text{Rank}(\mathbf{X}_l)\| * \|\text{Rank}(\mathbf{Y}_k) - \text{Rank}(\mathbf{Y}_m)\|. \end{aligned}$$

Let $\mathbf{x}_{\text{encode}} = (x_{\text{encode},1}, \dots, x_{\text{encode},h})^\top$ be the h -dimensional encoded data generated from the first step and $\mathbf{X} = (X_1, \dots, X_p)^\top \in \mathbb{R}^p$ be the original high-dimensional input feature. We compute the rank distance correlation between $\mathbf{x}_{\text{encode}}$ and each feature X_i as $\omega_i = \text{RdCorr}(X_i, \mathbf{x}_{\text{encode}})$ for $i = 1, \dots, p$, which measures the strength of dependence between X_i and $\mathbf{x}_{\text{encode}}$. Because $\mathbf{x}_{\text{encode}}$ extracts most of the information in the original features, ω_i can also be treated as a marginal utility to rank the importance of the features. In other words, the final selected k active features are the ones whose rank distance correlations are among the top k .

It is worthwhile to mention that this design also provides an estimation of the number of true active features. Let $\omega_{(1)} \leq \omega_{(2)} \leq \dots \leq \omega_{(p)}$ be the order statistics of ω s. Suppose \mathcal{M} is the

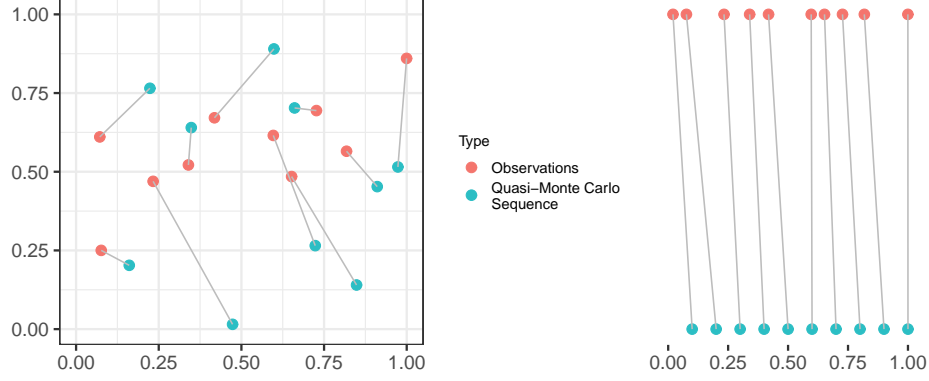


Fig. 1: *An illustration of multivariate rank. The red dots are the observed data points and blue dots are the “uniform like” quasi-Monte Carlo sequence on $[0,1]^2$. The (empirical) multivariate rank of each observation is the closest point in the quasi-Monte Carlo sequence.*

set of true active features with size $m_0 \leq p$. Apparently, $\hat{m} = \arg \max_{1 \leq i \leq p-1} \omega_{(i+1)}/\omega_{(i)}$ is an estimation of m_0 .

Figure 2 outlines the architecture of the feature extraction step and the feature screening step. Furthermore, we also summarize in Algorithm 1 the detailed procedure to carry out the proposed method.

4. NUMERICAL RESULTS

In this section, we conduct extensive simulation studies to examine the performance of the proposed feature screening method on synthetic datasets. To this end, we design four simulation experiments that correspond to four different scenarios: categorical response, continuous response, unknown structure, and unsupervised learning. Each simulation consists of 100 independent replications. Similar to Fan and Lv (2008), we choose the top $k = \lfloor n/\log(n) \rfloor$ features in all simulation designs, where $\lfloor a \rfloor$ denotes the integer part of a .

We also compare our method with some existing state-of-the-art methods. They are (1) the classical feature screening method, *iterative sure independence screening* (ISIS) of Fan and Lv

Algorithm 1: Deep Feature Screening

Input: input design matrix $\mathbf{X} \in \mathbb{R}^{n \times p}$, response vector $\mathbf{y} = (y_1, \dots, y_n)^\top$ (if available),encoder network Φ , decoder network Ψ , regressor or classifier Υ (if available),learning rate η , tuning parameter λ , number of epochs for the first step E **Step 1: Dimension Reduction and Feature Extraction**Initialize Θ .**for** $e \in \{1, \dots, E\}$ **do** $\hat{\mathbf{x}}_{\text{encode}} = \Phi(\mathbf{x})$ $\hat{\mathbf{y}} = \Upsilon(\hat{\mathbf{x}}_{\text{encode}})$ (if response is available) $\hat{\mathbf{x}} = \Psi(\hat{\mathbf{x}}_{\text{encode}})$ **if** *response is not available*: **then** $\mathcal{L} = \|\hat{\mathbf{x}} - \mathbf{x}\|_2^2$ **if** *response is continuous*: **then** \mathcal{L} is defined in (3.2) **if** *response is categorical*: **then** \mathcal{L} is defined in (3.3) Compute gradient of the loss \mathcal{L} w.r.t. Θ using backpropagation $\nabla_{\Theta} \mathcal{L}$ and update $\Theta \leftarrow \Theta - \eta \nabla_{\Theta} \mathcal{L}$.Finish Step 1 and obtain $\mathbf{x}_{\text{encode}} = \frac{\Phi(\mathbf{x}) - \min \Phi(\mathbf{x})}{\max \Phi(\mathbf{x}) - \min \Phi(\mathbf{x})} \in \mathbb{R}^h$.**Step 2: Feature Screening**Generate a Sobol sequence $\{\mathbf{c}_1, \dots, \mathbf{c}_n\} \subset [0, 1]^h$ **for** $i \in \{1, \dots, p\}$ **do** Compute rank distance correlation between the i -th feature X_i and $\mathbf{x}_{\text{encode}}$ $\omega_i = \text{RdCorr}(X_i, \mathbf{x}_{\text{encode}})$ using (3.4), (3.5), and (3.6).**return** feature importance scores

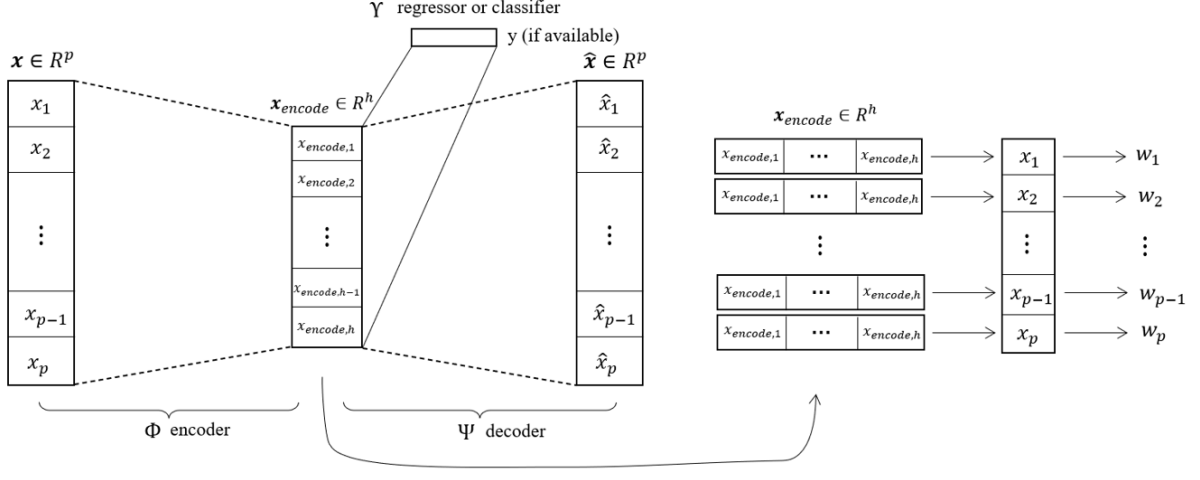


Fig. 2: The architecture DeepFS consists of an autoencoder based dimension reduction method for feature extraction (on the left) and a multivariate feature screening (on the right). $\mathbf{x}_{\text{encode}} \in \mathbb{R}^h$ is the low-dimensional representation of the original input which captures most of the information of the data in \mathbb{R}^p , where $h \ll p$, and is used to compute the strength of dependence with each feature.

(2008), (2) two Lasso-based (or ℓ_1 -regularized) algorithms, *PLasso* of Yang et al. (2020) and *LassoNet* of Lemhadri et al. (2021), (3) the reparametrization trick-based method, *concrete autoencoder* (CAE) of Abid et al. (2019), and (4) two two-step methods, *feature selection network* (FsNet) of Singh et al. (2020) and *teacher-student feature selection network* (TSFS) of Mirzaei et al. (2020). Among the six methods, LassoNet, CAE, FsNet, and TSFS are deep learning based.

In each simulation, we let \mathcal{J} denote the set of true active variables and $\hat{\mathcal{J}}_i$ the set of selected variables in the i -th replication. The following metric is used to evaluate the performance of each method:

$$\varrho = \frac{1}{100} \sum_{i=1}^{100} \frac{|\hat{\mathcal{J}}_i \cap \mathcal{J}|}{|\mathcal{J}|},$$

which measures the proportion of active variables selected out of the total amount of true active variables. Such metric has been widely used in feature selection literature (see Fan and Lv, 2008; Yang et al., 2020).

There are many hyper-parameters in our approach: the number of layers, the number of

neurons in each layer, dropout probability, learning rate, the tuning parameter λ in the loss function, and the dimensionality of the latent space \mathcal{F} . These hyper-parameters play an important role in our method. It can be difficult to assign values to the hyper-parameters without expert knowledge on the domain. In practice, it is common to use grid search, random search (Bergstra and Bengio, 2012), Bayesian optimization (Snoek et al., 2012), among others, to obtain optimal values of the hyper-parameters. In this paper we search for the desirable values of the hyper-parameters by minimizing the loss over the predefined parameter candidates using a validation set. As CAE is unsupervised, we follow the instruction in Abid et al. (2019) to adapt it to the supervised setting. For each simulation, we use the Adam optimizer to train the network.

4.1 Simulation 1: Categorical Response

In this simulation study, we consider the classification problem and suppose that the true relationship between the response and the features are complex and nonlinear. Inspired by the fact that high-dimension, low-sample-size data always occur in genome-wide association studies (GWAS) and gene selection, we follow the simulation design of GWAS feature selection in Wu et al. (2009) and Yang et al. (2020). Let $y \in \{0, 1\}$ be the binary response and $\mathbf{x} = (x_1, \dots, x_p)^\top$ be the single nucleotide polymorphisms (SNPs). The data are generated as follows. We first generate n independent auxiliary random vectors $\mathbf{Z}_i = (Z_{i1}, \dots, Z_{ip})^\top, i = 1, \dots, n$, from a multivariate Gaussian distribution $\mathcal{N}(0, \Sigma)$, where Σ is a $p \times p$ covariance matrix capturing the correlation between SNPs. The design of Σ is the same as Yang et al. (2020); that is,

$$\Sigma_{ij} = \begin{cases} 1 & \text{if } i = j, \\ \rho & \text{if } i \neq j, i, j \leq p/20, \\ 0 & \text{otherwise,} \end{cases} \quad (4.7)$$

with $\rho \in \{0, 0.5, 0.8\}$. This design enables closer SNPs to have a stronger correlation. Next, we randomly generate p minor allele frequencies (MAFs) m_1, \dots, m_p from uniform distribution $Uniform(0.05, 0.5)$ to represent the strength of heritability. For the i -th observation, $i = 1, \dots, n$,

the SNPs $\mathbf{x}_i = (x_{i1}, \dots, x_{ip})^\top$ are generated according to the following rule: for $j = 1, \dots, p$,

$$x_{ij} = \begin{cases} \epsilon & Z_{ij} \leq c_1, \\ \epsilon + 1 & c_1 < Z_{ij} < c_2, \\ \epsilon + 2 & Z_{ij} \geq c_2, \end{cases}$$

where ϵ is sampled from $\mathcal{N}(0, 0.1^2)$, and c_1 and c_2 are the $(1 - m_j)^2$ -quantile and $(1 - m_j^2)$ -quantile of $\{Z_{1j}, \dots, Z_{nj}\}$, respectively.

Suppose there are 10 (out of p) active SNPs associated with the response and let $J = \{j_1, \dots, j_{10}\}$, where $j_k, k = 1, \dots, 10$, are randomly sampled from $\{1, \dots, p\}$ without replacement. The response $y_i, i = 1, \dots, n$, is generated according to the dichotomous phenotype model

$$\begin{aligned} \log \frac{\pi_i}{1 - \pi_i} = & -3 + \beta_1 x_{i,j_1} + \beta_2 \sin(x_{i,j_2}) + \beta_3 \log(x_{i,j_3}^2 + 1) + \beta_4 x_{i,j_4}^2 \\ & + \beta_5 \mathbb{I}(x_{i,j_5} < 1) + \beta_6 \max(x_{i,j_6}, 1) + \beta_7 x_{i,j_7} \mathbb{I}(x_{i,j_7} < 0) \\ & + \beta_8 \sqrt{|x_{i,j_8}|} + \beta_9 \cos(x_{i,j_9}) + \beta_{10} \tanh(x_{i,j_{10}}), \end{aligned}$$

with $y_i \sim \text{Binomial}(1; \pi_i)$ and $\beta_j, j = 1, \dots, 10$, sampled from $\text{Uniform}(1, 2)$. To examine the effects of the sample size and the dimension on the accuracy of the feature selection procedure, we consider $n \in \{200, 500, 1000\}$ and $p \in \{1000, 3000\}$.

Table 1 reports, for various methods, the proportion of active variables selected out of 10 averaged over 100 replications and its standard error (displayed in parentheses) using different combinations of ρ, n , and p . It is evident that for all the feature selection methods, a large dimension and/or a strong dependence among the SNPs adversely affect the accuracy of the proposed method, and increasing the sample size always improves the selection accuracy. Table 1 also shows that our method outperforms other methods in all aspects.

4.2 Simulation 2: Continuous Response

In this experiment, we investigate the validity of our method when applied to continuous response. Because FsNet is designed for categorical response, to provide a fair comparison, we change the classifier to a regressor in the loss function of FsNet. In particular, we generate n independent

Table 1: Results of Simulation 1: the averaged ϱ over 100 replicates (with its standard error in parentheses) of various methods using different combinations of ρ , n , and p

ρ	(n, p)	ISIS	PLasso	CAE	FsNet	LassoNet	TSFS	DeepFS
0	(200, 1,000)	0.49 (0.07)	0.53 (0.05)	0.59 (0.06)	0.63 (0.05)	0.59 (0.06)	0.51 (0.07)	0.67 (0.05)
0	(500, 1,000)	0.51 (0.06)	0.64 (0.05)	0.68 (0.06)	0.72 (0.05)	0.69 (0.05)	0.56 (0.06)	0.76 (0.05)
0	(1,000, 1,000)	0.55 (0.06)	0.73 (0.04)	0.76 (0.05)	0.79 (0.04)	0.84 (0.05)	0.60 (0.07)	0.86 (0.04)
ρ	(n, p)	ISIS	PLasso	CAE	FsNet	LassoNet	TSTS	DeepFS
0	(200, 3,000)	0.37 (0.08)	0.44 (0.06)	0.52 (0.07)	0.57 (0.05)	0.54 (0.06)	0.40 (0.06)	0.61 (0.05)
0	(500, 3,000)	0.41 (0.07)	0.57 (0.05)	0.62 (0.06)	0.68 (0.06)	0.66 (0.05)	0.49 (0.07)	0.71 (0.05)
0	(1,000, 3,000)	0.44 (0.07)	0.65 (0.05)	0.70 (0.06)	0.72 (0.05)	0.73 (0.06)	0.57 (0.06)	0.79 (0.04)
ρ	(n, p)	ISIS	PLasso	CAE	FsNet	LassoNet	TSTS	DeepFS
0.5	(200, 1,000)	0.42 (0.07)	0.48 (0.06)	0.53 (0.07)	0.56 (0.05)	0.55 (0.04)	0.45 (0.05)	0.65 (0.06)
0.5	(500, 1,000)	0.45 (0.06)	0.59 (0.05)	0.63 (0.06)	0.68 (0.05)	0.67 (0.06)	0.53 (0.05)	0.74 (0.04)
0.5	(1,000, 1,000)	0.48 (0.07)	0.69 (0.05)	0.70 (0.07)	0.73 (0.04)	0.75 (0.05)	0.61 (0.06)	0.82 (0.05)
ρ	(n, p)	ISIS	PLasso	CAE	FsNet	LassoNet	TSTS	DeepFS
0.5	(200, 3,000)	0.33 (0.07)	0.41 (0.04)	0.49 (0.05)	0.53 (0.05)	0.49 (0.06)	0.38 (0.04)	0.57 (0.06)
0.5	(500, 3,000)	0.38 (0.07)	0.51 (0.05)	0.57 (0.06)	0.63 (0.06)	0.58 (0.07)	0.47 (0.05)	0.67 (0.06)
0.5	(1,000, 3,000)	0.41 (0.06)	0.59 (0.06)	0.64 (0.06)	0.69 (0.07)	0.68 (0.08)	0.56 (0.06)	0.74 (0.07)
ρ	(n, p)	ISIS	PLasso	CAE	FsNet	LassoNet	TSTS	DeepFS
0.8	(200, 1,000)	0.35 (0.07)	0.44 (0.05)	0.52 (0.05)	0.55 (0.05)	0.52 (0.06)	0.40 (0.04)	0.58 (0.06)
0.8	(500, 1,000)	0.41 (0.07)	0.53 (0.06)	0.58 (0.06)	0.65 (0.06)	0.61 (0.07)	0.48 (0.06)	0.68 (0.06)
0.8	(1,000, 1,000)	0.44 (0.08)	0.61 (0.06)	0.65 (0.07)	0.72 (0.08)	0.70 (0.09)	0.53 (0.06)	0.76 (0.08)
ρ	(n, p)	ISIS	PLasso	CAE	FsNet	LassoNet	TSTS	DeepFS
0.8	(200, 3,000)	0.29 (0.05)	0.35 (0.04)	0.44 (0.04)	0.48 (0.04)	0.44 (0.05)	0.32 (0.03)	0.51 (0.05)
0.8	(500, 3,000)	0.34 (0.05)	0.42 (0.04)	0.51 (0.04)	0.52 (0.05)	0.52 (0.05)	0.38 (0.04)	0.61 (0.06)
0.8	(1,000, 3,000)	0.37 (0.06)	0.49 (0.05)	0.58 (0.05)	0.57 (0.05)	0.61 (0.06)	0.42 (0.05)	0.67 (0.06)

random vectors $\mathbf{x}_i = (x_{i1}, \dots, x_{ip})^\top$ from a multivariate Cauchy distribution with mean zero and covariance matrix $\Sigma_{p \times p} = (\sigma_{ij})_{p \times p}$, with $\sigma_{ij} = \rho^{|i-j|}$. The response variable y_i is generated from

$$y_i = \beta_1 x_{i,j_1} + \beta_2 x_{i,j_2}^2 + \beta_3 x_{i,j_3} x_{i,j_4} + \beta_3 x_{i,j_5} x_{i,j_6} + \beta_4 \mathbb{1}(x_{i,j_6} < 0) + \epsilon_i,$$

where $\beta_1, \beta_2, \beta_3, \beta_4 \sim \text{Uniform}(1, 2)$, $j_k, k = 1, \dots, 6$, are sampled from $\{1, \dots, p\}$ without replacement, and $\epsilon_i \stackrel{iid}{\sim} \mathcal{N}(0, 1)$ is the error term. So in this experiment, there are 6 active features. Same as Simulation 1, we take $\rho \in \{0, 0.5, 0.8\}$, $n \in \{200, 500, 1000\}$, and $p \in \{1000, 3000\}$. The results are summarized in Table 2 and suggest that DeepFS is the best among all the methods, consistent with the results shown in Table 1.

4.3 Simulation 3: Unknown Structure

In this simulation, we consider the *Breast Cancer Coimbra Data Set* from UCI Machine Learning Repository <https://archive.ics.uci.edu/ml/datasets/\Breast+Cancer+Coimbra>. The dataset consists of 9 quantitative predictors (or features) and a binary response, indicating the presence or absence of breast cancer, with a total of $n = 116$ observations.

Note that the true relationship between the response and the predictors is unknown and can be complex and it is reasonable to assume that these 9 predictors have a strong association with the response. The following procedure is adopted in order to effectively evaluate our method. We add $p - 9$ more irrelevant features from standard normal distribution which are independent of the response, with $p \in \{1000, 5000, 10000\}$. In other words, among all the p features, there are only 9 active features that are associated with the response, while all the others are irrelevant. The goal of this simulation is to check whether our method can correctly select these 9 features from a high-dimensional feature space.

We report in Table 3 the mean value of the statistic ϱ from 100 replications and its standard error for $p = 1000, 5000$, and 10000 . We note that all deep learning based methods (i.e., CAE, FsNet, LassoNet, TSFS, and DeepFS) work better than the classical feature selection methods

Table 2: Results of Simulation 2: the averaged ϱ over 100 replicates (with its standard error in parentheses) of various methods using different combinations of ρ , n , and p .

ρ	(n, p)	ISIS	PLasso	CAE	FsNet	LassoNet	TSFS	DeepFS
0	(200, 1,000)	0.43 (0.06)	0.44 (0.04)	0.37 (0.04)	0.41 (0.05)	0.39 (0.05)	0.40 (0.05)	0.57 (0.04)
0	(500, 1,000)	0.47 (0.06)	0.51 (0.05)	0.48 (0.06)	0.53 (0.05)	0.55 (0.03)	0.46 (0.05)	0.63 (0.04)
0	(1,000, 1,000)	0.53 (0.06)	0.57 (0.04)	0.58 (0.05)	0.62 (0.04)	0.64 (0.03)	0.52 (0.06)	0.69 (0.05)
ρ	(n, p)	ISIS	PLasso	CAE	FsNet	LassoNet	TSFS	DeepFS
0	(200, 3,000)	0.32 (0.05)	0.34 (0.04)	0.32 (0.05)	0.38 (0.05)	0.33 (0.05)	0.32 (0.05)	0.52 (0.05)
0	(500, 3,000)	0.36 (0.05)	0.41 (0.05)	0.39 (0.06)	0.46 (0.06)	0.44 (0.05)	0.39 (0.06)	0.57 (0.05)
0	(1,000, 3,000)	0.42 (0.07)	0.49 (0.06)	0.47 (0.06)	0.51 (0.06)	0.54 (0.04)	0.48 (0.07)	0.61 (0.05)
ρ	(n, p)	ISIS	PLasso	CAE	FsNet	LassoNet	TSFS	DeepFS
0.5	(200, 1,000)	0.35 (0.05)	0.37 (0.05)	0.36 (0.06)	0.37 (0.06)	0.35 (0.05)	0.31 (0.05)	0.53 (0.05)
0.5	(500, 1,000)	0.38 (0.06)	0.42 (0.06)	0.41 (0.08)	0.45 (0.07)	0.41 (0.07)	0.37 (0.07)	0.58 (0.06)
0.5	(1,000, 1,000)	0.43 (0.06)	0.48 (0.06)	0.45 (0.08)	0.49 (0.07)	0.51 (0.07)	0.50 (0.08)	0.63 (0.06)
ρ	(n, p)	ISIS	PLasso	CAE	FsNet	LassoNet	TSFS	DeepFS
0.5	(200, 3,000)	0.29 (0.04)	0.32 (0.04)	0.27 (0.05)	0.32 (0.05)	0.29 (0.05)	0.28 (0.05)	0.42 (0.05)
0.5	(500, 3,000)	0.32 (0.05)	0.37 (0.05)	0.34 (0.05)	0.41 (0.05)	0.37 (0.06)	0.35 (0.06)	0.49 (0.05)
0.5	(1,000, 3,000)	0.39 (0.06)	0.45 (0.07)	0.39 (0.06)	0.44 (0.05)	0.40 (0.06)	0.41 (0.06)	0.52 (0.06)
ρ	(n, p)	ISIS	PLasso	CAE	FsNet	LassoNet	TSFS	DeepFS
0.8	(200, 1,000)	0.30 (0.04)	0.33 (0.04)	0.31 (0.03)	0.33 (0.05)	0.31 (0.05)	0.30 (0.05)	0.48 (0.06)
0.8	(500, 1,000)	0.34 (0.04)	0.38 (0.05)	0.38 (0.04)	0.38 (0.05)	0.35 (0.05)	0.33 (0.06)	0.51 (0.06)
0.8	(1,000, 1,000)	0.39 (0.05)	0.42 (0.05)	0.41 (0.05)	0.41 (0.05)	0.47 (0.06)	0.40 (0.06)	0.58 (0.06)
ρ	(n, p)	ISIS	PLasso	CAE	FsNet	LassoNet	TSFS	DeepFS
0.8	(200, 3,000)	0.27 (0.03)	0.29 (0.03)	0.28 (0.03)	0.31 (0.05)	0.27 (0.04)	0.27 (0.04)	0.39 (0.04)
0.8	(500, 3,000)	0.30 (0.03)	0.34 (0.04)	0.33 (0.05)	0.38 (0.05)	0.35 (0.04)	0.33 (0.05)	0.43 (0.04)
0.8	(1,000, 3,000)	0.35 (0.04)	0.38 (0.04)	0.38 (0.05)	0.41 (0.05)	0.40 (0.05)	0.39 (0.05)	0.50 (0.05)

Table 3: Results of Simulation 3: the averaged ϱ over 100 replicates (with its standard error in parentheses) of various methods using different ps .

(n, p)	ISIS	PLasso	CAE	FsNet	LassoNet	TSFS	DeepFS
(116, 1,000)	0.18 (0.02)	0.19 (0.03)	0.28 (0.03)	0.26 (0.03)	0.32 (0.04)	0.57 (0.05)	0.60 (0.04)
(116, 5,000)	0.16 (0.03)	0.16 (0.03)	0.25 (0.02)	0.23 (0.02)	0.28 (0.04)	0.53 (0.03)	0.57 (0.04)
(116, 10,000)	0.12 (0.02)	0.16 (0.02)	0.23 (0.02)	0.21 (0.02)	0.23 (0.03)	0.51 (0.04)	0.53 (0.04)

(i.e., ISIS and PLasso), and our proposed method is more capable of selecting the right active features than the other four methods, regardless of the dimensionality.

4.4 Simulation 4: Unsupervised Learning

Our last simulation investigates the empirical performance of unsupervised learning. Suppose there are two classes of data with sample sizes $n_1 = n_2 = n$, and dimension p . The data in the two classes are drawn from two independent multivariate Gaussian distributions: $\mathcal{N}_p(\mathbf{0}_p, \mathbf{I}_p)$ for Class 1 and $\mathcal{N}_p(\boldsymbol{\mu}, \mathbf{I}_p)$ for Class 2, where $\mathbf{0}_p$ is a p dimensional vector of zeros, and \mathbf{I}_p is a $p \times p$ identity matrix. Moreover, $\boldsymbol{\mu}$ is a p dimensional vector with j_k -th element equal one for $k = 1, \dots, 10$ and the rest all being zeros, where j_k s are randomly sampled from $\{1, \dots, p\}$ without replacement. In other words, the mean vector in the second class has 10 non-zero values.

Again, we compute the selection precision statistic ϱ and its standard error with $n \in \{200, 500, 1000\}$ and $p \in \{1000, 3000\}$, as in Simulations 1 and 2, for all the methods based on 100 replications. The results are summarized in Table 4. Because ISIS and PLasso only work for supervised learning, we omit these two methods from analysis. The numerical results in Table 4 indicate the superiority of DeepFS in unsupervised feature selection setting.

Table 4: Results of Simulation 4: the averaged ϱ over 100 replicates (with its standard error in parentheses) of various methods using different combinations of ρ , n , and p .

(n, p)	ISIS	PLasso	CAE	FsNet	LassoNet	TSFS	DeepFS
(200, 1,000)	*	*	0.57	0.62	0.61	0.65	0.69
	*	*	(0.06)	(0.07)	(0.06)	(0.07)	(0.06)
(500, 1,000)	*	*	0.68	0.73	0.76	0.78	0.81
	*	*	(0.06)	(0.07)	(0.07)	(0.07)	(0.07)
(1,000, 1,000)	*	*	0.79	0.81	0.82	0.85	0.87
	*	*	(0.07)	(0.08)	(0.07)	(0.07)	(0.08)
(n, p)	ISIS	PLasso	CAE	FsNet	LassoNet	TSFS	DeepFS
(200, 3,000)	*	*	0.46	0.48	0.52	0.57	0.61
	*	*	(0.04)	(0.05)	(0.04)	(0.05)	(0.06)
(500, 3,000)	*	*	0.55	0.59	0.63	0.66	0.73
	*	*	(0.04)	(0.05)	(0.04)	(0.06)	(0.06)
(1,000, 3,000)	*	*	0.61	0.66	0.72	0.76	0.80
	*	*	(0.05)	(0.06)	(0.05)	(0.07)	(0.06)

5. REAL DATA ANALYSIS

In this section, we illustrate the usefulness of the proposed feature selection method by applying it to real-world problems. We introduce the datasets and evaluation metrics in Section 5.1 and present the empirical findings in Section 5.2.

5.1 Datasets and Metrics

We consider four datasets that feature high dimension and low sample size and can be found at <https://jundong1.github.io/scikit-feature>.

- **Colon.** The colon tissues data consist of gene expression differences between tumor and normal colon tissues measured in $p = 2000$ genes, where 20 samples are from normal group and 42 samples are from tumor tissues.
- **Leukemia.** The Leukemia data are a benchmark dataset for high-dimensional data analysis which contains two classes of samples, the acute lymphoblastic leukaemia group and acute myeloid leukaemia group, with observations 47 and 25 respectively. The dimensionality of the dataset is $p = 7070$.

Table 5: Summary of the four datasets used in Section 5.

Dataset	Colon	Leukemia	Prostate Cancer	CLL.SUB
Sample Size	62	72	102	111
Dimensionality	2000	7070	6033	11340
Number of Classes	2	2	2	3

- **Prostate Cancer.** The prostate cancer dataset contains genetic expression levels for $p = 6033$ genes with sample size 102, in which 50 are normal control subjects and 52 are prostate cancer patients.
- **CLL.SUB.** The CLL.SUB dataset has gene expressions from high density oligonucleotide arrays containing genetically and clinically distinct subgroups of B-cell chronic lymphocytic leukemia. The dataset consists of $p = 11340$ attributes, 111 instances, and 3 classes.

A brief summary of the four datasets is provided in Table 5. For each dataset, we run various feature selection algorithms to select the top k features, with k varying from 10 to 150, and the dimensionality h of the latent space \mathcal{F} is chosen as 5 (its adequacy will be justified later via a sensitivity analysis). Their performance is evaluated using two criteria: classification accuracy and reconstruction error, which are also considered in Mirzaei et al. (2020), Lemhadri et al. (2021), and Singh et al. (2020). In order to assess classification accuracy, we use the selected features as the input for a downstream classifiers: a single-layer feed-forward neural network. The classification accuracy is measured on the test set. Regarding the reconstruction error, we reconstruct the original data using the selected features and a single-layer feed-forward neural network, and define the reconstruction error as the mean square error between the original and the reconstructed ones.

5.2 Results

We divide each dataset randomly into training, validation, and test sets with a 70-20-10 split. We use the training set to learn the parameters of the autoencoders, the validation set to select opti-

mal hyper-parameters, and the test set to evaluate the generalization performance. We repeat the entire process 10 times, and each time we compute the statistics using the three aforementioned criteria. We then average these statistics across the 10 experiments. As CAE is unsupervised, we add a softmax layer to its loss function.

In Figure 3, we plot the classification accuracy as a function of k , the number of selected features. In comparison with the other methods, for all the four datasets, DeepFS has a higher classification accuracy regardless of the value of k and a faster convergence rate as k increases. In particular, our method yields a much higher classification accuracy when the number of selected features is small. These suggest that the features selected by DeepFS are more informative. Figure 4 shows the results of reconstruction error against the number of selected features. It is evident that DeepFS is the best performer among all the methods across all the datasets. Moreover, Figures 3 and 4 indicate that the deep learning based methods (i.e., DeepFS, FsNet, CAE, LassoNet, and TSFS) overall have a better performance than classical feature selection algorithms (i.e., ISIS and PLasso).

In DeepFS, the dimensionality h of the latent space \mathcal{F} (i.e., the dimensionality of $\mathbf{x}_{\text{encode}}$) is a hyper-parameter and controls the relative accuracy between the feature extraction step and feature screening step. While a higher value of h helps extract more information from the autoencoder, it results in a larger variance in the estimation of multivariate rank distance correlation. Hence, we perform a sensitivity analysis that investigates the effect of h on the performance of DeepFS. Figure 5 depicts the classification accuracy as k increases from 10 to 150 with $h = 5, 10$, and 15. There is almost no difference among the three curves associated with different values of h , suggesting that DeepFS is insensitive to the choice of h .

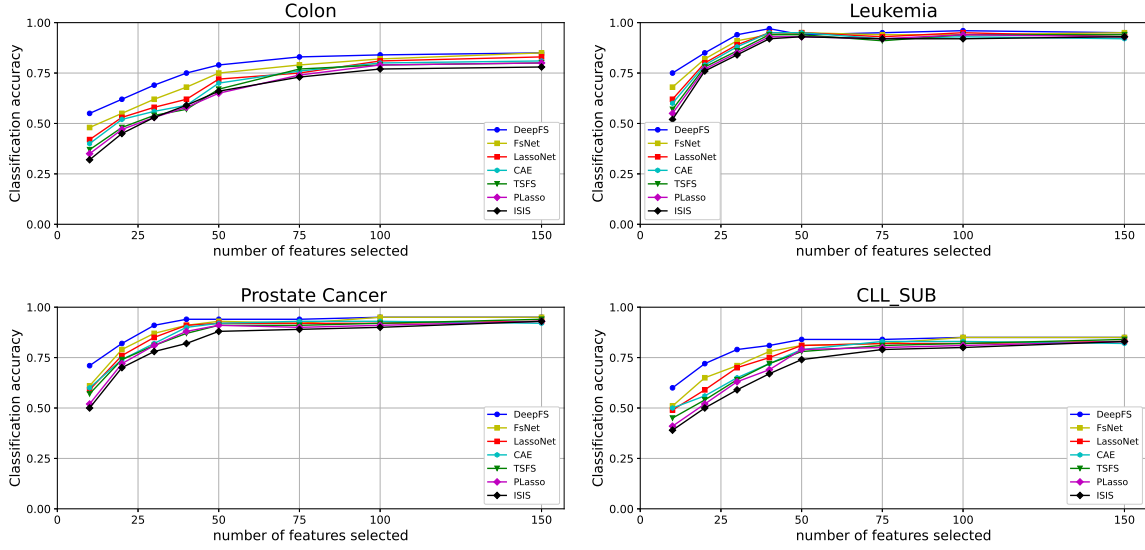


Fig. 3: A comparison of classification accuracy among various methods. For each method, we use a single hidden layer neural network with ReLU active function for classification. All reported values are on a hold-out test set.

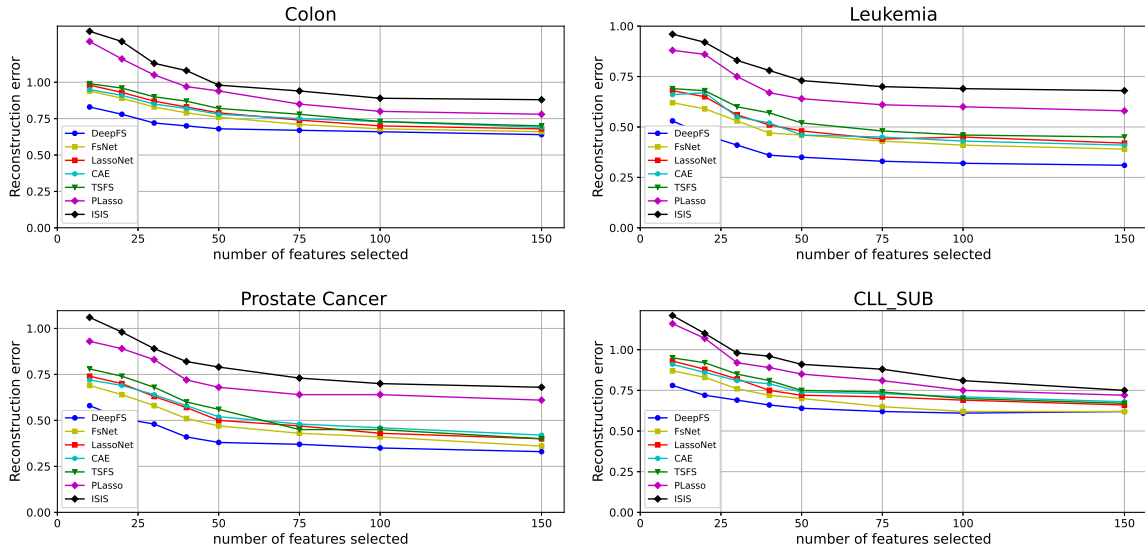


Fig. 4: A comparison of reconstruction error among various methods. For each method, a single hidden layer neural network with ReLU active function is employed to reconstruct the original input. All reported values are on a hold-out test set.

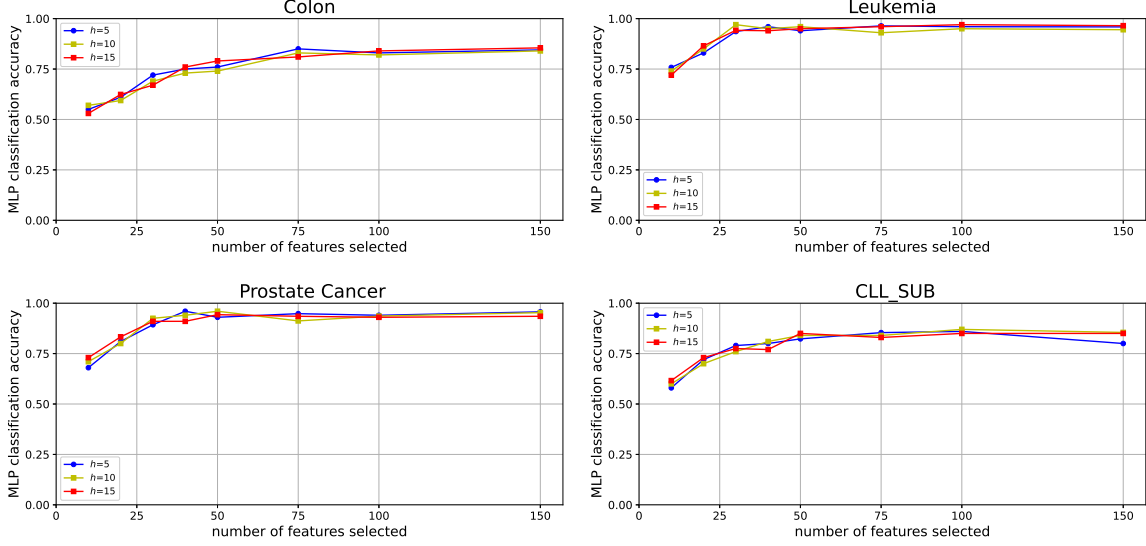


Fig. 5: Sensitivity analysis of the dimensionality of $\mathbf{x}_{\text{encode}}$.

6. CONCLUSION

In this paper, we proposed a new framework named DeepFS that novelly combines deep learning and feature screening for feature selection under high-dimension, low-sample-size setting. DeepFS consists of two steps: a deep neural network for feature extraction and a multivariate feature screening for feature selection. DeepFS enjoys both advantages of deep learning and feature screening. Unlike most other feature screening methods, DeepFS takes into account both interactions among features and reconstruction of the original input, owing to the deep neural network in the first step. Moreover, DeepFS is applicable to both unsupervised and supervised settings with continuous or categorical responses.

In this work, we use an autoencoder for feature extraction, which can be easily adapted to other methods, such as convolutional neural network. In the future, we plan to use more sophisticated network architectures in replace of autoencoder and theoretically prove sure screening property.

REFERENCES

- Abid, A., Balin, M. F., and Zou, J. (2019). Concrete autoencoders for differentiable feature selection and reconstruction. *arXiv preprint arXiv:1901.09346*.
- Amaldi, E. and Kann, V. (1998). On the approximability of minimizing nonzero variables or unsatisfied relations in linear systems. *Theoretical Computer Science*, 209(1):237–260.
- Bahdanau, D., Cho, K., and Bengio, Y. (2014). Neural machine translation by jointly learning to align and translate. *arXiv preprint arXiv:1409.0473*.
- Bergstra, J. and Bengio, Y. (2012). Random search for hyper-parameter optimization. *Journal of Machine Learning Research*, 13(10):281–305.
- Chandrashekar, G. and Sahin, F. (2014). A survey on feature selection methods. *Computers & Electrical Engineering*, 40(1):16–28. 40th-year commemorative issue.
- Deb, N. and Sen, B. (2021). Multivariate rank-based distribution-free nonparametric testing using measure transportation. *Journal of the American Statistical Association*, pages 1–16.
- Ding, C. H. (2003). Unsupervised feature selection via two-way ordering in gene expression analysis. *Bioinformatics*, 19(10):1259–1266.
- Fan, J. and Lv, J. (2008). Sure independence screening for ultrahigh dimensional feature space. *Journal of the Royal Statistical Society: Series B (Statistical Methodology)*, 70(5):849–911.
- Fan, J., Samworth, R., and Wu, Y. (2009). Ultrahigh dimensional feature selection: beyond the linear model. *The Journal of Machine Learning Research*, 10:2013–2038.
- Farrell, M. H., Liang, T., and Misra, S. (2021). Deep neural networks for estimation and inference. *Econometrica*, 89(1):181–213.

- Feng, S. and Duarte, M. F. (2018). Graph autoencoder-based unsupervised feature selection with broad and local data structure preservation. *Neurocomputing*, 312:310–323.
- Halton, J. and Smith, G. (1964). Radical inverse quasi-random point sequence, algorithm 247. *Commun. ACM*, 7(12):701.
- Han, K., Wang, Y., Zhang, C., Li, C., and Xu, C. (2018). Autoencoder inspired unsupervised feature selection. In *2018 IEEE International Conference on Acoustics, Speech and Signal Processing (ICASSP)*, pages 2941–2945.
- He, K., Zhang, X., Ren, S., and Sun, J. (2016). Deep residual learning for image recognition. In *Proceedings of the IEEE conference on computer vision and pattern recognition*, pages 770–778.
- Jang, E., Gu, S., and Poole, B. (2016). Categorical reparameterization with gumbel-softmax. *arXiv preprint arXiv:1611.01144*.
- Jiménez-Luna, J., Grisoni, F., and Schneider, G. (2020). Drug discovery with explainable artificial intelligence. *Nature Machine Intelligence*, 2(10):573–584.
- Kabir, M. M., Shahjahan, M., and Murase, K. (2011). A new local search based hybrid genetic algorithm for feature selection. *Neurocomputing*, 74(17):2914–2928.
- Khalid, S., Khalil, T., and Nasreen, S. (2014). A survey of feature selection and feature extraction techniques in machine learning. In *2014 Science and Information Conference*, pages 372–378.
- Kumar, V. and Minz, S. (2014). Feature selection: a literature review. *SmartCR*, 4(3):211–229.
- Lemhadri, I., Ruan, F., Abraham, L., and Tibshirani, R. (2021). LassoNet: A neural network with feature sparsity. *Journal of Machine Learning Research*, 22(127):1–29.
- Li, K., Wang, F., Liu, R., Yang, F., and Shang, Z. (2021). Calibrating multi-dimensional complex ode from noisy data via deep neural networks. *arXiv preprint arXiv:2106.03591*.

- Li, R., Zhong, W., and Zhu, L. (2012). Feature screening via distance correlation learning. *Journal of the American Statistical Association*, 107(499):1129–1139.
- Li, Y., Chen, C.-Y., and Wasserman, W. W. (2016). Deep feature selection: theory and application to identify enhancers and promoters. *Journal of Computational Biology*, 23(5):322–336.
- Liu, B., Wei, Y., Zhang, Y., and Yang, Q. (2017). Deep neural networks for high dimension, low sample size data. In *IJCAI*, pages 2287–2293.
- Liu, R., Boukai, B., and Shang, Z. (2022). Optimal nonparametric inference via deep neural network. *Journal of Mathematical Analysis and Applications*, 505(2):125561.
- Liu, R., Shang, Z., and Cheng, G. (2020). On deep instrumental variables estimate.
- Miao, J. and Niu, L. (2016). A survey on feature selection. *Procedia Computer Science*, 91:919–926. Promoting Business Analytics and Quantitative Management of Technology: 4th International Conference on Information Technology and Quantitative Management (ITQM 2016).
- Mirzaei, A., Mohsenzadeh, Y., and Sheikhzadeh, H. (2017). Variational relevant sample-feature machine: a fully bayesian approach for embedded feature selection. *Neurocomputing*, 241:181–190.
- Mirzaei, A., Pourahmadi, V., Soltani, M., and Sheikhzadeh, H. (2020). Deep feature selection using a teacher-student network. *Neurocomputing*, 383:396–408.
- Mohsenzadeh, Y., Sheikhzadeh, H., and Nazari, S. (2016). Incremental relevance sample-feature machine: A fast marginal likelihood maximization approach for joint feature selection and classification. *Pattern Recognition*, 60:835–848.
- Qi, M., Wang, T., Liu, F., Zhang, B., Wang, J., and Yi, Y. (2018). Unsupervised feature selection by regularized matrix factorization. *Neurocomputing*, 273:593–610.

- Saeys, Y., Inza, I., and Larranaga, P. (2007). A review of feature selection techniques in bioinformatics. *Bioinformatics*, 23(19):2507–2517.
- Scardapane, S., Comminiello, D., Hussain, A., and Uncini, A. (2017). Group sparse regularization for deep neural networks. *Neurocomputing*, 241:81–89.
- Schmidt-Hieber, J. (2020). Nonparametric regression using deep neural networks with relu activation function. *The Annals of Statistics*, 48(4):1875–1897.
- Singh, D., Climente-González, H., Petrovich, M., Kawakami, E., and Yamada, M. (2020). Fsnet: Feature selection network on high-dimensional biological data. *arXiv preprint arXiv:2001.08322*.
- Snoek, J., Larochelle, H., and Adams, R. P. (2012). Practical bayesian optimization of machine learning algorithms. *Advances in neural information processing systems*, 25.
- Sobol’, I. M. (1967). On the distribution of points in a cube and the approximate evaluation of integrals. *Zhurnal Vychislitel’noi Matematiki i Matematicheskoi Fiziki*, 7(4):784–802.
- Solorio-Fernández, S., Carrasco-Ochoa, J. A., and Martínez-Trinidad, J. F. (2020). A review of unsupervised feature selection methods. *Artificial Intelligence Review*, 53(2):907–948.
- Taherkhani, A., Cosma, G., and McGinnity, T. M. (2018). Deep-fs: A feature selection algorithm for deep boltzmann machines. *Neurocomputing*, 322:22–37.
- Varshavsky, R., Gottlieb, A., Linial, M., and Horn, D. (2006). Novel Unsupervised Feature Filtering of Biological Data. *Bioinformatics*, 22(14):e507–e513.
- Wang, S., Cao, G., Shang, Z., and Initiative, A. D. N. (2021). Estimation of the mean function of functional data via deep neural networks. *Stat*, 10(1):e393.

- Wu, T. T., Chen, Y. F., Hastie, T., Sobel, E., and Lange, K. (2009). Genome-wide association analysis by lasso penalized logistic regression. *Bioinformatics*, 25(6):714–721.
- Yang, S., Wen, J., Eckert, S. T., Wang, Y., Liu, D. J., Wu, R., Li, R., and Zhan, X. (2020). Prioritizing genetic variants in GWAS with lasso using permutation-assisted tuning. *Bioinformatics*, 36(12):3811–3817.
- Zhao, S. and Fu, G. (2021). Distribution-free and model-free multivariate feature screening via multivariate rank distance correlation. *arXiv preprint arXiv:2110.03145*.
- Zhu, P., Xu, Q., Hu, Q., and Zhang, C. (2018). Co-regularized unsupervised feature selection. *Neurocomputing*, 275:2855–2863.

□